Physiological and Molecular Plant Pathology 133 (2024) 102343

Contents lists available at ScienceDirect

Physiological and Molecular Plant Pathology

journal homepage: www.elsevier.com/locate/pmpp

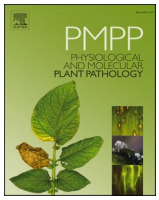

Identification of effector candidates in *Bipolaris sorokiniana* and their expression profile analysis during pathogen-wheat interactions

Mahla Kamajian, Aboozar Soorni *, Rahim Mehrabi **

Department of Biotechnology, College of Agriculture, Isfahan University of Technology, Isfahan, Iran

ARTICLE INFO

Keywords:
B. sorokiniana
Spot blotch
Effector proteins
Gene expression
Structural similarity

ABSTRACT

Spot blotch disease, caused by the fungal pathogen *Bipolaris sorokiniana*, poses a significant threat to global production particularly wheat, and barley due to substantial yield losses. Similar to many fungal pathogens, the infection of host plants heavily depends on the pathogen's ability to secrete effector proteins, which manipulate host defenses and aid disease progression. However, a critical knowledge gap exists in the comprehensive identification and characterization of effector candidates (ECs) in *B. sorokiniana*, requiring further research efforts. Therefore, study aimed to systematically identify and characterize ECs in *B. sorokiniana* by conducting pathogenicity tests to confirm disease symptoms on wheat leaves, utilizing a rigorous bioinformatics approach to predict ECs through sequence analysis and structural similarities, and validating effector expression profiles during infection using RNA sequencing (RNA-Seq) and quantitative real-time polymerase chain reaction (qRT-PCR). Pathogenicity testing confirmed the typical symptoms of spot blotch disease upon inoculation with *B. sorokiniana*. Through bioinformatics analysis, 81 ECs were identified, showing dynamic expression patterns during infection stages. Among these ECs, genes such as Cocsa1|129517, Cocsa1|141231, and Cocsa1|193443 stood out due to their different expression patterns and structural similarities, indicating their potential roles as effectors. This study offers new novel insights into the effector repertoire of *B. sorokiniana* and its implications for spot blotch disease management. The identified ECs present promising targets for further investigation to clarify their specific roles in fungal virulence and host immune modulation.

1. Introduction

B. sorokiniana, also known as *Cochliobolus sativus* in its teleomorph form, is significant phytopathogenic fungus that affects a wild range of hosts across different genera and families, causing various destructive diseases such as wheat root rot, crown rot, leaf spot, spot blotch, and black points in different cereals like wheat and barley [1–3]. The impact of these diseases on wheat cultivation is substantial, with common root rot, for example, leading to significant yield losses in various wheat-growing regions. For example, in Canada between 1969 and 1971, common root rot resulted in approximately 5.7 % wheat loss, amounting to $42 million [4]. Similarly, crown rot caused by *B. sorokiniana* in the Pacific Northwest has been estimated to cause up to 35 % yield loss in wheat [5]. Spot blotch is the most significant disease caused by *B. sorokiniana*, and poses a substantial threat to wheat and barley cultivation, particularly in warm regions, where losses can range from 15 % to 25 % [6]. Additionally, seed infection by *B. sorokiniana* can lead to black point disease, impacting seed quality and potentially contributing to root rot and seedling blight [7,8].

Plants have developed defense mechanisms against pathogens to reduce pathogen damage, but pathogens have also evolved sophisticated strategies to circumvent these defenses by secreting effectors and metabolites. These effectors fall into two main categories: the host cell cytosol and the apoplastic space [9,10]. While oomycetes utilize conserved motifs like RxLR for effector entry [11], fungal effectors exhibit less uniformity, although certain motifs such as Y/F/WxC have been identified [12]. The majority of fungal effectors lack conserved domains, indicating their diverse mechanisms [13,14]. Convergent evolution has resulted in the targeting of a common host protein network by effectors from various pathogens, indicating a conserved mechanism of effector action across different microbial kingdoms [15]. Moreover, effector proteins can either induce or suppress plant immune responses, often leading to cell death or immune activation [16,17]. Certain effectors are specifically recognized by plant resistance proteins,

* Corresponding author.
** Corresponding author.
E-mail addresses: soorni@iut.ac.ir (A. Soorni), mehrabi@iut.ac.ir (R. Mehrabi).

https://doi.org/10.1016/j.pmpp.2024.102343
Received 24 April 2024; Received in revised form 12 June 2024; Accepted 17 June 2024
Available online 17 June 2024

termed avirulence proteins, triggering a robust immune response in the host plant [18]. For example, avirulence proteins like AvrPrm3 in *Blumeria graminis* and Avr2 and Avr3 in *Fusarium oxysporum* interact with corresponding resistance genes, impacting disease resistance breeding programs [19,20].

Given the critical importance of effectors in the pathogenicity of plant pathogens like *B. sorokiniana*, the identification of these effectors is paramount for devising effective disease management strategies. Consequently, few studies have been conducted to gain insights into the repertoire of effectors utilized by *B. sorokiniana*. For example, Condon et al. (2013) conducted a comparative analysis of candidate effector-coding genes across five *Bipolaris* species, identifying 289 putative small-molecular-weight secreted proteins in *B. sorokiniana* [21]. Pathak et al. (2020) further delved into this area by investigating the secretome of 196 proteins predicted to be present in *B. sorokiniana* through silico analysis [22]. Notably, Sudhir et al. (2020) identified the ToxA gene, which encodes a host-selective toxin functioning as an effector, within *B. sorokiniana*, shedding light on specific effector mechanisms employed by this pathogen [23]. In a recent study, a putative secreted protein, CsSp1, was identified as being induced during the early stages of infection. Through genetic manipulation, CsSP1 was found to play a critical role in fungal growth, spore production, and pathogenicity in wheat. Furthermore, functional analysis revealed CsSp1's ability to suppress lesion formation caused by *Phytophthora capsici*, suggesting its importance in modulating host immune responses. Intriguingly, CsSp1 was observed to localize within both the nucleus and cytoplasm of plant cells, indicating its multifaceted role in host-pathogen interactions [24].

Despite previous research efforts, there remains a gap in effectively identifying effectors in *B. sorokiniana* using robust bioinformatics approaches and experimental validation such as expression analysis. To fill this gap, we designed the current study to comprehensively identify putative effectors in *B. sorokiniana* and validate their expression patterns. Our study employed a rigorous bioinformatics pipeline to filter and select candidate effectors based on specific criteria, followed by experimental validation using RNA-Seq data and qRT-PCR analysis. Through this integrated approach, we obtained insightful results that contribute to a better understanding of effector-mediated pathogenicity in *B. sorokiniana*, thus filling a crucial gap in the existing literature.

2. Material and methods

2.1. Isolation and purification of B. sorokiniana

The isolation and purification procedure of *B. sorokiniana* started with collecting leaf samples exhibiting spot blotch, sourced from Golestan (Table 1). These samples underwent a preliminary treatment with 1 % sodium hypochlorite for 2–3 min. Subsequently, the treated leaf samples were subjected to three consecutive washes with sterile distilled water. The prepared samples were maintained on the moist filter paper at 20 °C. Upon the appearance of conidiophore and conidia of *B. sorokiniana*, the conidia were collected from the leaves and then evenly spread on a water-agar culture medium, with a composition of 15 g of agar per liter of culture medium. Following an incubation period of approximately 5–8 h, germinated conidia were transferred to peptone sucrose agar (PSA) culture medium (Fig. 1). Notable, we previously confirmed that the isolate used in this study produces ToxA by using BsToxA specific primers, following the methodology outlined in McDonald et al. (2018) [25].

Table 1
Geographic information of *B. sorokiniana* isolates collected in golestan.

Isolate	region	Location code	Isolate code	Latitude	Longitude
B. sorokiniana	Golestan-Bandar-e Gaz	loc2-a	90M2AB5S1	36.48911	52.77124

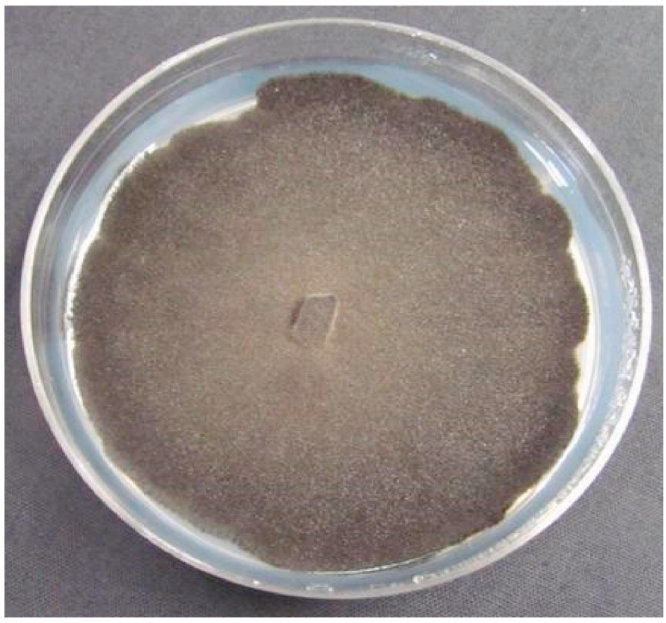

Fig. 1. The conidia of *B. sorokiniana* transferred to PSA culture medium.

2.2. Pathogenicity test, inoculation and sampling

The pathogenicity test was conducted by inoculating seedlings of the susceptible Darab 2 wheat cultivar. Darab 2, classified as *Triticum aestivum*, has been previously identified as a susceptible cultivar [26]. In this regard, the PSA culture medium was incubated in dark conditions at a temperature of 22 °C for 8 days. Then, the concentration of the resulting conidial suspension was determined using a slide hemocytometer and adjusted to 5 x 10^6 per ml amended with 0.15 % Tween 20. Inoculation was carried out by applying the spore suspension onto 15-day-old plants using a hand sprayer. = Subsequently, the inoculated seedlings underwent 24 h of darkness in conditions of saturated humidity, under transparent nylon covers. This experimental setup maintained a temperature range of 20–22 °C with alternating cycles of 12 h of light and 12 h of darkness. Leaf sampling was conducted at specific time points: before treatment (referred to as time 0: control) and subsequently at 1, 2, 3, 4, 5, and 7 days post-inoculation (DPI). The collected leaf samples were carefully enveloped in aluminum foil, immediately frozen in liquid nitrogen, and then stored at −80 °C for subsequent RNA extraction procedures.

2.3. Starvation test

The investigation into nutrient deprivation utilized a minimal culture medium to mimic conditions similar to the pathogen's early stages of attacking the plant during pathogenicity, where limited nutritional resources are available. To achieve this, the culture medium B5 (Gamborg) was prepared for experimentation. For the mycelium starvation test, mycelia were transferred to B5 culture medium, with three distinct treatments: 1) absence of a nitrogen source (B5–N), 2) absence of a carbon source (B5–C), and 3) absence of both nitrogen and carbon sources (B5–N, C).

2.4. Identification and selection of ECs

According to the availability of the *B. sorokiniana* genome on JGI website (https://mycocosm.jgi.doe.gov/Cocsa1/Cocsa1.home.html), the protein sequences corresponding to the genes were acquired from

the aforementioned database. After data retrieval, a systematic process was executed to filter and select candidate genes, involving the following steps.

1. Selection of proteins with a size of less than 300 amino acids.
2. Utilization of SignalP v.3.0 [27] software (http://www.cbs.dtu.dk/services/SignalP-3.0/) to identify secreted proteins. This method relies on the integration of artificial neural networks and hidden Markov models (HMM) to predict cleavage sites and the presence or absence of peptide signals [28].
3. Identification and removal of proteins containing N-terminal sequences, such as mitochondrial target peptide (mTP), chloroplast transition peptide (cTP) through TargetP v1.01 software (http://www.cbs.dtu.dk/services/TargetP-1.0/) [29].
4. Recognition and elimination of membrane proteins using TMHMM v.2.0 software (http://www.cbs.dtu.dk/services/TMHMM/) [30].
5. Employment of Big_PI (http://mendel.imp.ac.at/gpi/fungi_server.html) to exclude proteins attached to the cell wall. This software is proficient in identifying and removing proteins featuring a GPI anchor [31].
6. Manual selection of proteins containing 6 or more cysteine amino acids.
7. Assessment of the presence or absence of the remaining proteins in other fungi through homology search. Subsequently, functional investigation of the proteins was carried out using Pfam (http://pfam.xfam.org/) and InterPro (https://www.ebi.ac.uk/interpro/) software [32,33].
8. Utilization of the EffectorP 2.0 website (http://effectorp.csiro.au/) to predict fungal effectors [34].
9. Implementation of LOCOLIZER (http://localizer.csiro.au/) to determine the localization of effector proteins in plant cells [35].

2.5. RNA-seq data analysis

The assessment of expression for identified ECs involved the retrieval and analysis of RNA-Seq data from the European Nucleotide Archive (ENA) accessible through the BioProject accession numbers PRJNA743515 (https://www.ebi.ac.uk/ena). The previous study has described sampling, RNA extraction, and sequencing methods [24]. Briefly, in this study, wheat cultivar Aikang 58, a cultivar known to be susceptible to *B. sorokiniana*, verified in previous research [3,24,36], was utilized as the experimental subject. Aikang 58 samples were subjected to infection with or without the B. sorokiniana WT strain Lankao 9-3 at the seedling stage. The experimental conditions and procedures for the infection were previously reported by Kang et al. (2020) [36]. Specifically, clean stem bases and rootssamples were meticulously collected at two-time points, 5 and 15 days after inoculation for RNA extraction. Wheat RNA samples, each replicated twice, were subsequently sent to Novogene (Tianjin Novogene Bioinformatic Technology Co., Ltd) for sequencing.

The selected dataset underwent examination on the Galaxy website (https://usegalaxy.eu) [37]. Initial quality assessment of reads was performed using FastQC (v.0.11.8; https://www.bioinformatics.babraham.ac.uk/projects/fastqc/), followed by the removal of low-quality bases and adapter contamination through the application of the Trimmomatic tool v.0.38 [38]. Trimmomatic parameters included the pruning of bases with a quality score $<$ Q30 and the elimination of reads with lengths $<$50 bp. Subsequently, high-quality clean reads were mapped to the *B. sorokiniana* genome reference genome using STAR v2.7.10b [39]. The transcripts associated with the reference genome were assembled using StringTie v.2.1.1 [40]. Differential expression analysis on the gene read count data matrices was conducted with the assistance of the Python script prepDE.py. The generated matrices were uploaded to the IDEAMEX website [41] for analysis. DESeq2 [42] software was then employed to identify differentially expressed genes (DEGs), utilizing screening parameters of FDR $\leq$0.015, log2 fold change (logFC) $\geq$ 2, and CPM = 1.

2.6. Primer design

Following the identification of candidate genes, gene-specific primers were carefully designed to facilitate the examination of gene expression (Table 2). The primer design process involved the utilization of Oligo, Primer3 (http://primer3.ut.ee/), and IDT-OligoAnalyzer softwares (https://eu.idtdna.com/calc/analyzer). Subsequently, NCBIPrimer-BLAST software (http://www.ncbi.nlm.nih.gov/tools/primer-blast/) was employed to validate the primers' specificity. The designed primers exhibited a length ranging between 18 and 23 nucleotides, with a GC percentage falling within the range of 40–60 %. Furthermore, the optimal length of PCR product for qRT-PCR reactions was stipulated to range between 150 and 200 bp.

2.7. RNA extraction and cDNA synthesis

RNA isolation was executed using the CTAB extraction method [43]. To reduce potential variability arising from inter-individual inconsistencies in gene expression, leaves from three plants were collected, pooled and subjected to RNA extraction for each sample. The concentration and purity of extracted RNA were assessed using a NanoDrop Spectrophotometer (NanoDrop Technologies) and agarose gel electrophoresis. Subsequently, the RNA samples underwent quantification and the initiation of cDNA library preparation followed. In the context of reverse transcription quantitative polymerase chain reaction (RT-qPCR), the procedure commenced with the treatment of isolated RNA samples using DNase I enzyme to eliminate genomic DNA contamination. Specifically, 2 μg of total RNA was subjected to incubation with 1 U of DNase I (Thermo Fisher Scientific) at 37 °C for 30 min, followed by heat inactivation at 75 °C for 10 min. After this enzymatic treatment, the DNase I-treated RNA was subjected to reverse transcription using Moloney Murine Leukemia Virus Reverse Transcriptase (M-MLV RT). The reaction mixture, comprising 2 μg of DNase I-treated RNA, 200 U M-MLV RT, 500 μM dNTPs, 5 μM random hexamer primers, 10 mM DTT, and 20 U RNase inhibitor, was incubated at 37 °C for 1 h, followed by enzyme inactivation at 70 °C for 15 min.

2.8. qRT-PCR analysis

To validate the expression profiles of selected genes, qRT-PCR was

Table 2
Primer information for gene expression analysis.

Gene IDs		Primer sequence (5′–3′)	TM	Amplification length
Cocsa1| 117287	F	TTGGAAGAGGCACCAGAGAA	58.6	184
	R	GCTTCGAGAAGTCGATGTGG	58.7	
Cocsa1| 129976	F	CCAGAGCATCCCAAACTGTG	58	167
	R	ATGCCTTTCAAGCAGGACAA	59	
Cocsa1| 141231	F	TTGGCGATTTTGTTGACTGC	56.4	169
	R	GCAAGGAGAAAAACTACGCTGA	60	
Cocsa1| 181176	F	CTCTGGAAAGTGCCCGTATG	58.3	173
	R	GCTCCCGGAAATATGGTGAA	57.7	
Cocsa1| 125559	F	CAGCACAGGGCTCGATCA	60	181
	R	TGGGAAGTTGATTCCACAGG	60	
Cocsa1| 203267	F	AACCCCATTCACGCTCGTA	59	181
	R	GCGGGTTATCACTTCTTTAGCA	58.7	
Cocsa1| 193443	F	CCGCAGGGAGATCTGTATGA	58.7	194
	R	TCTCAGCACGGCAATCTACA	59	
Cocsa1| 131280	F	CACCGACAAGCTCCAGTGA	59.5	162
	R	TTCATGGGAAGTGTCCTTGC	58.4	
Cocsa1| 189555	F	TATTATGCCCCGAGGAGGAC	58.4	196
	R	CCGACTTTCAATCTTCGCAGT	58.9	
Cocsa1| 119439	F	GCCACCAGCATTACACATCC	59.3	179
	R	CAGATTGGCAACGGCTACG	59.3	
GAPDH	F	GGCAACGCTTAGGAGTCAGGA	62.1	118
	R	GCCTAGCCAGAAGTTCCGAGAAT	62.3	

employed for the quantitative evaluation of candidate gene expression in leaf tissues across diverse time points. In this further experiment, we used susceptible wheat cultivar Darab 2 for the qRT-PCR validation. This approach aimed to verify that the identified effector candidates are not cultivar-specific, thereby confirming their broader applicability. The use of different cultivars allowed us to ensure that the observed gene expression profiles are consistent across susceptible wheat varieties. The qRT-PCR experiments were conducted in a StepOne Real-Time PCR system, with a final reaction volume of 15 μL. This volume encompassed 7.5 μL of SYBR Green Master Mix (BioFACT, Korea), 2 μL of diluted cDNA, and 0.1 μL of each primer (10 pM), supplemented with PCR-grade water to reach the specified volume. The qRT-PCR protocol involved an initial denaturation step of 5 min at 95 °C, followed by 40 cycles consisting of 10 s at 95 °C, 20 s at the primer-specific annealing temperature, and 20 s at 72 °C, concluding with a melting curve program. The subsequent statistical analysis of gene expression adhered to the $2^{-\Delta\Delta Ct}$ method [44,45], employing *GADPH* as the internal reference (housekeeping) gene.

2.9. Structural modeling of EC

In this regard, the EC protein tertiary structures were predicted utilizing the Swiss model. The prediction focused on the most highly expressed EC members. Subsequently, the predicted EC protein tertiary structures underwent screening against the RCSB PDB database using the Dali server [46] to identify proteins with analogous folds. Hits with a Z-score of ≥2 were considered as having significant similarity. The alignment and visualization of protein tertiary structures were carried out using PyMol v2.5, along with the alignment plugin tool CEalign [47]. To explore similarities further, the TM-align method [48] was employed to calculate the root-mean-square deviation (RMSD) value. Lastly, the investigation into the general fold of confidently predicted protein tertiary structures was conducted using RUPEE [49,50], comparing them against the SCOPe v2.08 database [51]. Proteins identified with a knottin fold in the SCOPe database underwent assessment using Knotter 3D to ascertain the presence of a genuine knottin structure.

3. Results

3.1. Pathogenicity test

The outcomes of the pathogenicity test elucidated the pathogen responsible for the spot blotch disease, demonstrating its capacity to induce characteristic symptoms. Initial symptoms appeared 48 h post-inoculation as localized green islands gradually turned into chlorotic spots. Over time, these chlorotic areas gradually expanded and darkened, transitioning into necrotic spots as the infection progressed. Ultimately, seven days post-inoculation, necrotic lesions coalesced together, covering the majority of the leaf area and forming extended blotches, which constitute a signature symptom of the disease (Fig. 2).

3.2. Identification of ECs

To identify ECs, first, a total number of 12,250 genes was obtained from *B. sorokiniana* isolate ND90Pr genome. After the exclusion of proteins exceeding 300 amino acids length, a subset of 4758 proteins was derived. SignalP v.3.0 software facilitated the identification of 491 secreted proteins. Through the utilization of TargetP v1.01 software, 39 proteins characterized by an N-terminal presequence were identified and subsequently excluded. The application of Big-PI for the removal of cell wall-associated proteins resulted in the exclusion of 48 proteins. Employing TMHMM v.2.0 software revealed 49 membrane proteins, which were also excluded. Manual calculation of cysteine amino acids within mature proteins led to the selection of proteins containing 6 or more cysteine amino acids. Following preliminary analysis, a final set of 81 secreted proteins, possessing the desired characteristics, was identified (Table S1).

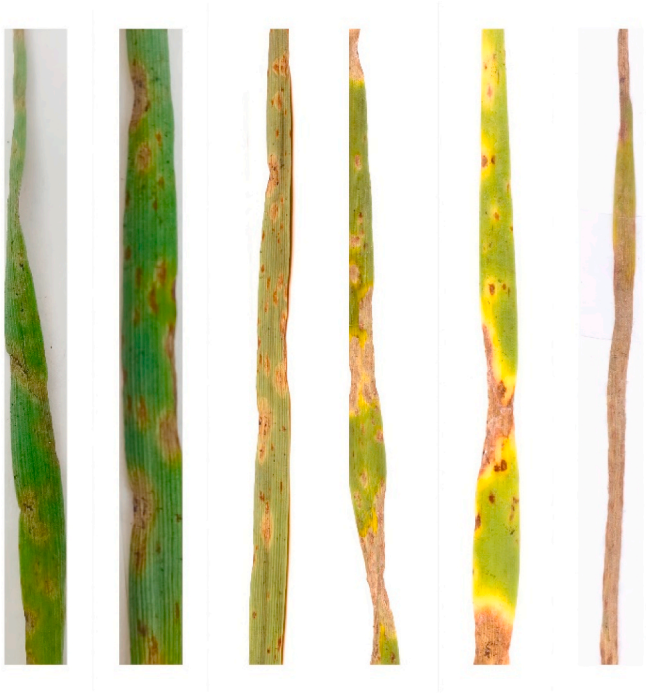

Fig. 2. The progression of disease stages and the development of burn spots caused by *B. sorokiniana* observed (from left to right) on the first, second, third, fourth, fifth, and seventh days after inoculation.

3.3. Evaluation of ECs expression using RNAseq data

Based on the findings derived from the analysis of gene expression, a total of 391 differentially expressed genes (DEGs) were detected, out of which five, including Cocsa1|166818, Cocsa1|116197, Cocsa1|182966,

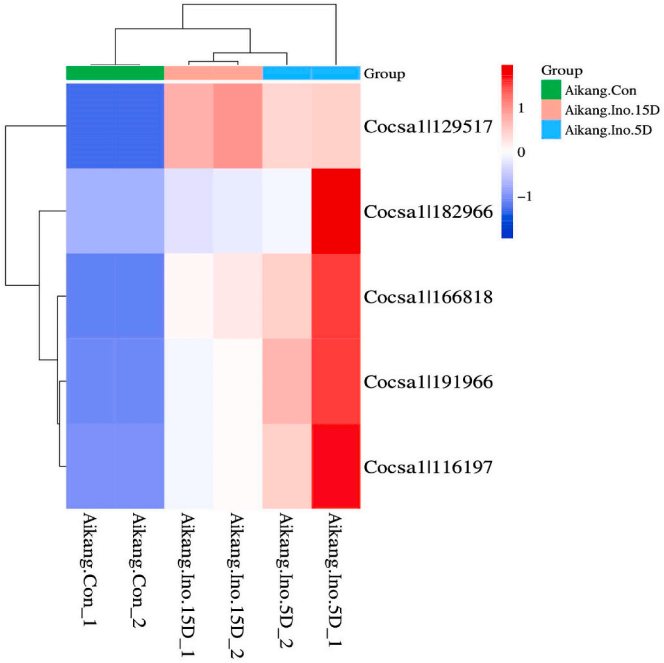

Fig. 3. Heatmap illustrating the expression levels of five ECs identified as DEGs through RNA-Seq data analysis.

Cocsa1|191966, and Cocsa1|129517, were found to be among the 81 ECs identified through the bioinformatics pipeline (Fig. 3). The transcriptional analysis conducted in this study revealed intricate patterns in gene expression across three different experimental conditions: Aikang.Con (pre-inoculation), Aikang.Ino.5D (post-inoculation after 5 days), and Aikang.Ino.15D (post-inoculation after 15 days). The transcripts that were identified, distinguished by their unique identifiers, displayed significant changes in their expression levels. Notably, Cocsa1|116197 exhibited the highest level of expression after 5 days of inoculation, while Cocsa1|182966 showed the lowest expression level during the same time. After 15 days, all genes, except for Cocsa1|129517, demonstrated a decrease in their expression levels.

3.4. Gene expression profile using qRT-PCR

Gene expression analysis was conducted using qRT-PCR to evaluate five additional newly identified ECs. The analysis was performed in three replicates each for biological and technical purposes. The samples

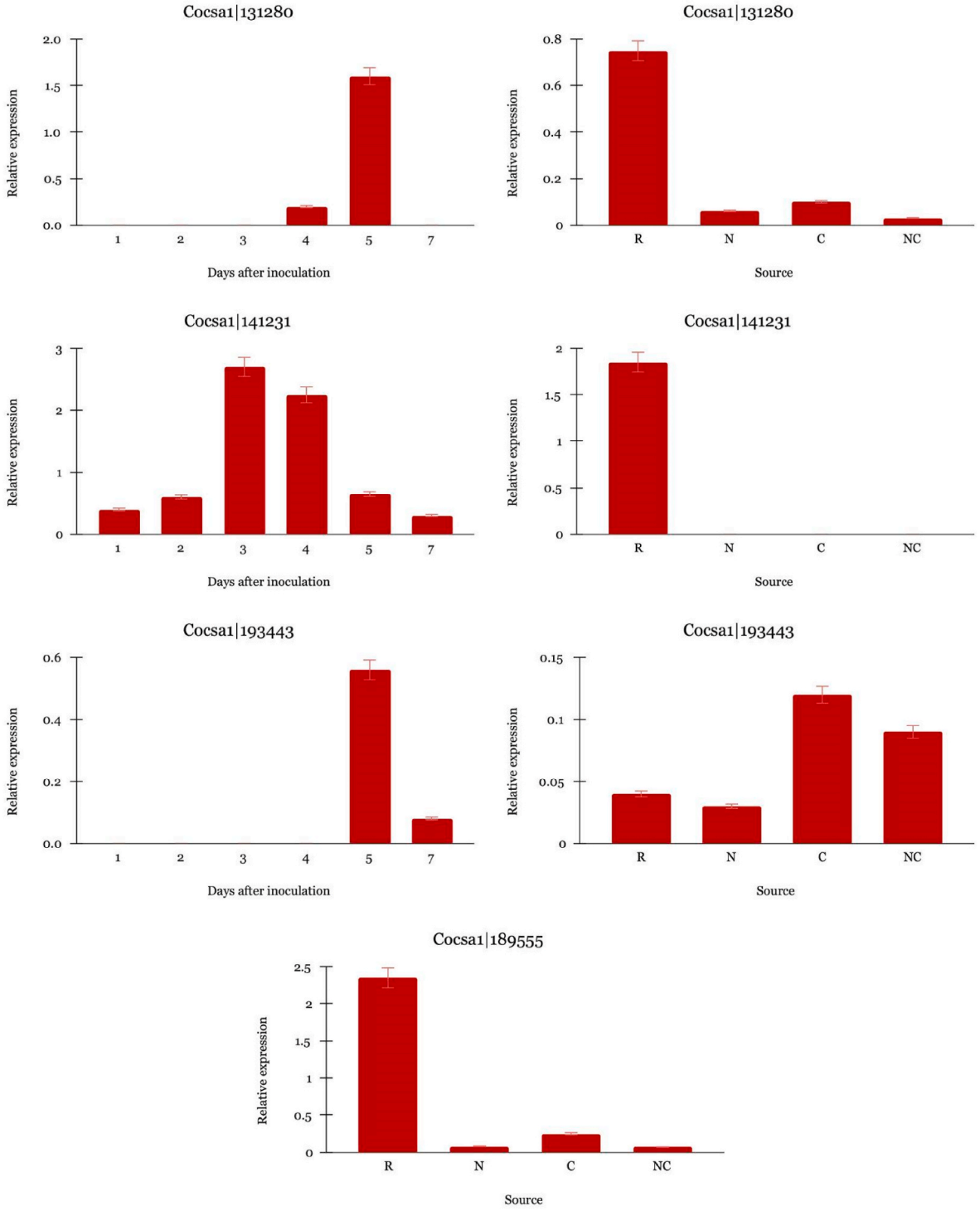

Fig. 4. Relative expression of five ECs at intervals of 1, 2, 3, 4, 5, and 7 days after inoculation with *B. sorokiniana* and samples subjected to the mycelium starvation test.

were divided into two distinct groups for analysis (Fig. 4). The first group consisted of wheat leaves collected at intervals of 1, 2, 3, 4, 5, and 7 days after inoculation with *B. sorokiniana*. The second group comprised samples subjected to the mycelium starvation test. This approach allowed for a comprehensive evaluation of the ECs, as it encompassed four different levels of analysis. However, Cocsa1|117287 gene did not exhibit a proprietary amplification, rendering it unsuitable for further analysis and subsequently excluded from the study. Besides, Cocsa1|189555 did not indicate any expression during all time points.

The temporal expression pattern of Cocsa1|141231 gene, among those evaluated, exhibited a dynamic profile. Initially, at 1 day post-inoculation, the expression level was relatively low. However, there was a noticeable increase in gene expression at 2 dpi, followed by a substantial increase at 3 dpi. The expression levels remained relatively high at 4 dpi before declining at 5 and 7 dpi. On the other hand, the Cocsa1|131280 gene did not show any expression at the early time points (1, 2, and 3 dpi), but there was a notable increase at 4 dpi, reaching its peak expression at 5 dpi. Subsequently, the expression levels returned to baseline at 7 dpi. In contrast, the Bs9 gene displayed minimal expression throughout the early time points (1–4 days) and exhibited a substantial increase at 5 dpi, followed by a slight decrease at 7 dpi. These observed expression dynamics suggest that Cocsa1|131280 and Cocsa1|193443 genes exhibit a responsive behavior during the later stages of infection. Notably, the analysis of these gene expressions in the RNA-Seq data revealed a noteworthy rise in the expression levels of Cocsa1|141231, Cocsa1|189555, and Cocsa1|117287 from 5 days post-inoculation to 15 days (Fig. 5). However, the expression of Cocsa1|131280 and Cocsa1|193443 did not exhibit consistent expression during the inoculation period.

In further investigation, the gene expression profiles of four genes were assessed under varying nutrient conditions, including a rich nutrient source (B5), absence of nitrogen (B5–N), absence of carbon (B5–C), and absence of both nitrogen and carbon (B5–N,C). Cocsa1|141231 exhibited a significant upregulation in expression under conditions of nitrogen and carbon deprivation, suggesting a regulatory role influenced by these nutrients. Conversely, Cocsa1|189555 displayed heightened expression in the rich nutrient source, while experiencing notable downregulation in nutrient-deprived conditions, indicating a dependence on nitrogen and carbon availability. Cocsa1|131280 exhibited had a low expression, particularly in the absence of both nitrogen and carbon sources, highlighting its sensitivity to nutrient variations. Cocsa1|193443 displayed relatively low expression levels across all conditions, with a modest increase in the absence of carbon.

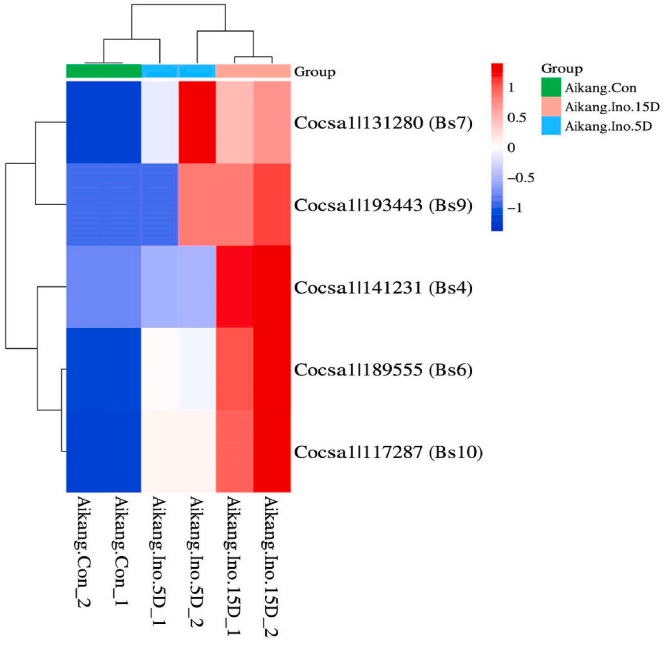

Fig. 5. Heatmap illustrating the expression levels (in RNA-Seq data) of five ECs evaluated by qRT-PCR.

3.5. Predicted structural similarity to other effector proteins

To understand the potential roles of ECs, we utilized the Swiss-model to predict their three-dimensional structures. Subsequently, we compared these structures with known proteins of characterized tertiary structures, and in certain instances, their functions, using the Dali server. Notably, this investigation focused particularly on the most abundantly expressed ECs. Interestingly, some ECs exhibited structural similarity to one or more ECs or Avr effector proteins from different plant-pathogenic fungi, whose tertiary structures have been elucidated. The structural examination identified a significant similarity between Cocsa1|129517 and AVRA6, AVRA10, and AVRA22 from *Blumeria graminis* f. sp. Hordei, with a z-score of approximately 5 and an RMSD of about 2.2. Additionally, a similarity was observed with an RNase-like effector from the fungal pathogen *B. graminis*, with a z-score of 4.3 and an RMSD of 2.9. It is important to note that despite sharing similar topology, these proteins exhibited substantial diversity at the amino acid level, with a maximum sequence identity of 15 %. Cocsa1|141231 was also found to exhibit structural similarity to the LysM effector known as EXTRACELLULAR PROTEIN 6 (Ecp6) originating from *Fulvia fulva,* displaying a z-score of 18.9, RMSD of 1.58, and a notable identity percentage of 36 %. Cocsa1|193443 was anticipated to exhibit structural homology with Avr3 (SIX1) sourced from *Fusarium oxysporum* f. sp. *lycopersici*, with a calculated z-score of 3.2 and RMSD of 4.55. Furthermore, through structural analysis, it was determined that Cocsa1|117287 displayed a remarkable structural similarity to LECTIN-C (C-type lectin effectors). This was supported by a strong z-score of 5.9 and a RMSD of 4.1. Importantly, the alignment of their sequences unveiled a substantial 32 % identity, providing additional evidence for their structural similarity.

4. Discussion

The significance of *B. sorokiniana* in cereal cultivation, especially in wheat production cannot be overstated, as it is responsible for a range of diseases including root rot, crown rot, leaf spot, and black point [7,52,53]. These diseases have substantial economic implications, leading to significant yield losses in various wheat-growing regions [2]. Despite previous research efforts yielding valuable insights into putative effectors [22–24], proteins pivotal in the pathogenicity of plant pathogens by modulating host defense mechanisms, our current understanding remains inadequate. Hence, the adoption of robust bioinformatics methodologies, coupled with rigorous experimental validation, is imperative to achieve a comprehensive identification and characterization of ECs in *B. sorokiniana*. Therefore, we utilized an advanced and accurate systematic bioinformatics pipeline to pinpoint potential ECs in *B. sorokiniana*. While several computational pipelines have been devised to predict fungal secretomes, including Secretool [54], Fungal Secretome Database (FSD) [55], FunSecKB [56], FunSecKB2 [57], and Aspertome [58], the pipeline by Mueller et al. (2008) offers a refined approach [59]VVM. Thus, we utilized the Mueller et al. (2008) pipeline with several modifications to augment its effectiveness in predicting secretory proteins in *B. sorokiniana*. These pipelines offer rapid predictions of potential secretory proteins, providing valuable insights into the secretomes of various fungi.

Based on our pipeline, a total of 81 ECs were detected, out of which 33 were found to align with the findings reported by Pathak et al., in 2020. It is noteworthy that our approach differed from that of Pathak et al. (2020) in several aspects. Specifically, while Pathak et al. relied on a criterion based on the presence of more than 5 cysteines, we imposed a more stringent threshold requiring the presence of more than 6 cysteines

in our analysis. Furthermore, Pathak et al. (2020) did not utilize the EffectorP 2.0 website (http://effectorp.csiro.au/) for predicting fungal effectors within secretory proteins, a tool that we incorporated into our methodology. Additionally, we employed LOCOLIZER (http://localizer.csiro.au/) to evaluate the localization of effector proteins, instead of ProtComp [60] undertaken in the study conducted by Pathak et al. (2020). Further investigation for the 81 ECs identified in our study revealed compelling findings. Through a comprehensive analysis, we conducted a BLASTp search against the fungi secretome database [61], which significantly hitted for 73 out of the 81 ECs. These hits underscored the potential relevance of these ECs as secreted proteins within the fungal kingdom. Upon comparison with the predicted secretome from FunSecKB2, all 73 ECs that showed significant hits in the fungal secretome database were designated as "highly likely" secreted proteins with WoLF PSORT scores ranging between 17 and 27. This alignment between our identified ECs and the highly probable secreted proteins in FunSecKB2 further validates the robustness of our computational approach in predicting fungal secreted proteins.

In addition to robust and accurate bioinformatic analysis, expression validation serves as a crucial step in confirming the findings. In our study, we applied two expression methods, RNA-Seq and qRT-PCR, to validate the results obtained through bioinformatics. Intriguingly, five of ECs were identified *via* the RNA-seq data analysis [24] as highly expressed genes during wheat leaf infection with *B. sorokiniana*. Interestingly, among these five ECs, Cocsa1|129517 exhibited structural similarity with previously identified effector proteins from *B. graminis* [19,62], a fungal pathogen known to cause powdery mildew disease in various cereal crops. The structural examination of *B. graminis* AVR effector proteins, including AVR_{A10}, AVR_{A22}, and AVR_{A6}, show a common structural scaffold shared among these effector proteins, characterized by two β-sheets and a central α-helix. The first β-sheet is composed of two or three anti-parallel β-strands, with two contributing to an N-terminal β-hairpin in AVR_{A10}, AVR_{A22}, and AVR_{A6}, while another β-strand is located at the very C-terminus of these proteins. The second β-sheet comprises three or four antiparallel β-strands, with at least two packing against the α-helix to stabilize the conformation of the β-sheet [63]. The structural similarity of Cocsa1|129517 with *B. graminis* AVR effectors implicates its potential involvement in host-pathogen interactions and fungal virulence. The conserved structural features observed in Cocsa1|129517, including the presence of key residues such as the Y/F/WxC-motif [12,64], suggested a possible role in stabilizing the common RNase-like effector family (RALPH) fold shared by these effectors. In cereal powdery mildew (PM) fungi, an extreme expansion of an RNase-like effector family, termed RALPH, dominates the effector repertoire, with some members recognized as avirulence (AVR) effectors by cereal NLR receptors [63]. The observed structural similarity between Cocsa1|129517 and an RNase-like effector from the fungal pathogen *B. graminis* provides further evidence supporting its potential association with the RALPH. The significant structural resemblance, as indicated by a z-score of 4.3 and an RMSD of 2.9, suggests a common structural scaffold shared between Cocsa1|129517 and the RNase-like effector from *B. graminis*. Thus, the structural comparison supports the notion that Cocsa1|129517 may indeed belong to the RALPH effector family, contributing to the understanding of its potential role in fungal pathogenesis and host-pathogen interactions.

In addition to employing RNA-Seq, we complemented our study by evaluating gene expression using qRT-PCR, thereby enhancing the robustness of our findings. Through this approach, several genes exhibited significant responses to infection, such as Cocsa1|141231. Our analysis revealed a dynamic expression pattern for Cocsa1|141231, characterized by a gradual increase in expression from 1 to 3 days post-inoculation, reaching peak levels at 4 dpi before declining towards the later time points (5 and 7 dpi). Furthermore, structural analysis unveiled striking similarities between Cocsa1|141231 and the well-characterized effector protein Ecp6 originating from *F. fulva*. Turning to Ecp6, it serves as a pivotal chitin-binding effector in *F. fulva*, crucial for evading recognition by host immune receptors and suppressing chitin-triggered immune responses in tomato plants [65,66]. Ecp6 achieves this by sequestering chito-oligosaccharides released from fungal hyphae, thereby preventing their recognition by extracellular chitin-binding receptors on the plant cell surface. Structural studies have elucidated the mechanism underlying Ecp6-mediated chitin sequestration, revealing intrachain dimerization of its lysin motif (LysM) domains, particularly domains 1 and 3, which mediate chitin binding. Additionally, LysM domain 2, although not directly involved in sequestration, has been implicated in perturbing chitin-triggered immune responses [67–69]. Moreover, the presence of LysM domains in Ecp6, along with its homologs found throughout the fungal kingdom, underscores the fundamental role of chitin scavenging in fungal pathogenicity [65,70]. The wide occurrence of LysM effectors in various fungal pathogens highlights their significance in modulating host immune responses and promoting fungal infection. The proteins containing the LysM domain that act as virulence factors through interactions with chitin were previously identified in the secretome of *B. sorokiniana* [71]. Interestingly, recent investigations by Pathack et al. (2020) identified three ECs, including jgi|Cocsa1|28281, jgi|Cocsa1|156991, and jgi|Cocsa1|141231, containing the LysM domain, with only jgi|Cocsa1|141231 being identified in our study. Given the structural similarity observed between Cocsa1|141231 and Ecp6, and the established role of Ecp6 in fungal pathogenesis and host-pathogen interactions, it raises intriguing possibilities regarding Cocsa1|141231 function as a potential effector. Indeed, the identification of Cocsa1|141231 as a putative EC underscores the importance of further research to elucidate its precise role in fungal pathogenesis and host immune evasion mechanisms.

Our integrated bioinformatic and expression analysis highlighted Cocsa1|193443 as another significant player among ECs in our study. This gene exhibited distinct expression dynamics during infection, particularly showing a responsive behavior during the later stages of the infection process. Notably, the analysis of these gene expressions in the RNA-Seq data revealed a noteworthy rise in the expression levels of Cocsa1|141231, Cocsa1|189555, and Cocsa1|117287 from 5 days post-inoculation to 15 days. Besides, structural analysis further revealed that Cocsa1|193443 shares homology with Avr3 (SIX1) sourced from *F. oxysporum* f. sp. *lycopersici*. Avr3 is a well-characterized effector protein that plays a pivotal role in the interaction between the fungus and its host plant, particularly in eliciting effector-triggered immunity (ETI) and disease resistance. Avr3, along with other effectors such as Avr1 (SIX4) and Avr2 (SIX3), is recognized by tomato immunity receptors (I, I-2, and I-3, respectively), leading to the activation of ETI and subsequent disease resistance [20,72]. The Avr3 protein comprises distinct structural domains that contribute to its function in host-pathogen interactions. Specifically, Avr3 consists of an N-terminal domain (N-domain) and a C-terminal domain (C-domain), each exhibiting unique structural features. The N-domain of Avr3 comprises an N-terminal α-helix followed by five β-strands, while the C-domain adopts a β-sandwich architecture involving seven or eight β-strands. Moreover, Avr3 exhibits a unique two-domain fold, representing a new structural class of fungal effectors termed the FOLD effectors. This distinctive structural arrangement is essential for the role of Avr3 in modulating host immune responses and promoting fungal infection. The functional significance of Avr3 in fungal pathogenesis and host immune evasion mechanisms highlights its importance as a key virulence factor in *F. oxysporum* f. sp. *lycopersici* [73–75]. Moreover, it is noteworthy that Cocsa1|193443 was also identified in a previous study by Pathack et al. (2020), further supporting its potential significance as an EC [22]. This convergence of evidence underscores the importance of further investigation into Cocsa1|193443 to elucidate its precise function in fungal pathogenesis and host immune modulation. Understanding the role of Cocsa1|193443 may offer valuable insights into developing effective strategies for disease management and crop protection against fungal pathogens.

5. Conclusion

In conclusion, through a combination of pathogenicity assay, bioinformatics analysis, and expression profiling, we identified a set of 81 secreted proteins coupled with experimental validation in fungal pathogenesis. Notably, several ECs, including Cocsa1|129517, Cocsa1|141231, and Cocsa1|193443, exhibited significant responses to infection and demonstrated structural homology with characterized effectors, suggesting their potential involvement in modulating host immune responses. By elucidating the precise pathogenesis, we can develop effective control measures for disease management, ensuring sustainable wheat production and global food security.

Funding

No funding was received for conducting this study.

Ethics approval and consent to participate

Not applicable.

Consent for publication

Not applicable.

CRediT authorship contribution statement

Mahla Kamajian: Writing – review & editing, Methodology, Investigation, Formal analysis, Conceptualization. **Aboozar Soorni:** Writing – review & editing, Writing – original draft, Visualization, Validation, Project administration, Methodology, Investigation, Formal analysis, Conceptualization. **Rahim Mehrabi:** Writing – review & editing, Project administration, Methodology, Investigation, Funding acquisition.

Declaration of competing interest

The authors declare no conflicts of interest.

Data availability

Data will be made available on request.

Appendix A. Supplementary data

Supplementary data to this article can be found online at https://doi.org/10.1016/j.pmpp.2024.102343.

References

[1] K. Acharya, A. Dutta, P. Pradhan, *Bipolaris sorokiana* (Sacc.) Shoem.: the most destructive wheat fungal pathogen in the warmer areas, Aust. J. Crop. Sci. 5 (2011) 1064–1071.
[2] S. KumarScholar, N. Kumar, S. Prajapati, Maurya, Review on Spot Blotch of Wheat: an Emerging Threat to Wheat Basket in Changing Climate, vol. 2, 2020, pp. 1985–1997.
[3] L. Minyan, W. Xiaoming, R. Xu, Y. Dongfang, H. Li, Root and leaf infection as revealed by autofluorescent reporter protein GFP labeled *Bipolaris sorokiniana* in wheat(利用绿色荧光蛋白报告基因标记研究麦根腐平脐孺孢 对小麦根和叶片的侵染), Sci. Agric. Sin. 17 (2012) 3506–3514, https://doi.org/10.3864/j.issn.0578-1752.2012.17.006.
[4] R.J. Ledingham, T.G. Atkinson, J.S. Horricks, J.T. Mills, L.J. Piening, R.D. Tinline, Wheat losses due to common root rot in the prairie provinces of Canada, 1969-71, Can, Plant Dis. Surv 53 (1973) 113–122.
[5] R.W. Smiley, J.A. Gourlie, S.A. Easley, L.-M. Patterson, R.G. Whittaker, Crop damage estimates for crown rot of wheat and barley in the Pacific Northwest, Plant Dis. 89 (2005) 595–604, https://doi.org/10.1094/PD-89-0595.
[6] P. Gupta, N. Vasistha, R. Aggarwal, A. Joshi, Biology of *B. sorokiniana* (syn. *Cochliobolus sativus*) in genomics era, J. Plant Biochem. Biotechnol. 27 (2017), https://doi.org/10.1007/s13562-017-0426-6.
[7] A.M. Al-Sadi, Bipolaris sorokiniana-induced black point, common root rot, and spot blotch diseases of wheat: a review, Front. Cell. Infect. Microbiol. 11 (2021) 584899, https://doi.org/10.3389/fcimb.2021.584899.
[8] Q.-Y. Li, Q.-Q. Xu, Y.-M. Jiang, J.-S. Niu, K.-G. Xu, R.-S. He, The correlation between wheat black point and agronomic traits in the North China Plain, Crop Protect. 119 (2019) 17–23, https://doi.org/10.1016/j.cropro.2019.01.004.
[9] M.C. Giraldo, B. Valent, Filamentous plant pathogen effectors in action, Nat. Rev. Microbiol. 11 (2013) 800–814, https://doi.org/10.1038/nrmicro3119.
[10] S. Zhang, J.-R. Xu, Effectors and effector delivery in magnaporthe oryzae, PLoS Pathog. 10 (2014) e1003826, https://doi.org/10.1371/journal.ppat.1003826.
[11] R.H.Y. Jiang, S. Tripathy, F. Govers, B.M. Tyler, RXLR effector reservoir in two *Phytophthora* species is dominated by a single rapidly evolving superfamily with more than 700 members, Proc. Natl. Acad. Sci. U.S.A. 105 (2008) 4874–4879, https://doi.org/10.1073/pnas.0709303105.
[12] D. Godfrey, H. Böhlenius, C. Pedersen, Z. Zhang, J. Emmersen, H. Thordal-Christensen, Powdery mildew fungal effector candidates share N-terminal Y/F/WxC-motif, BMC Genom. 11 (2010) 317, https://doi.org/10.1186/1471-2164-11-317.
[13] M.-C. Caillaud, S.J.M. Piquerez, G. Fabro, J. Steinbrenner, N. Ishaque, J. Beynon, J. D.G. Jones, Subcellular localization of the Hpa RxLR effector repertoire identifies a tonoplast-associated protein HaRxL17 that confers enhanced plant susceptibility, Plant J. 69 (2012) 252–265, https://doi.org/10.1111/j.1365-313X.2011.04787.x.
[14] C. Selin, T.R. de Kievit, M.F. Belmonte, W.G.D. Fernando, Elucidating the role of effectors in plant-fungal interactions: progress and challenges, Front. Microbiol. 7 (2016) 600, https://doi.org/10.3389/fmicb.2016.00600.
[15] R. Weßling, P. Epple, S. Altmann, Y. He, L. Yang, S.R. Henz, N. McDonald, K. Wiley, K.C. Bader, C. Gläßer, M.S. Mukhtar, S. Haigis, L. Ghamsari, A.E. Stephens, J. R. Ecker, M. Vidal, J.D.G. Jones, K.F.X. Mayer, E. Ver Loren van Themaat, D. Weigel, P. Schulze-Lefert, J.L. Dangl, R. Panstruga, P. Braun, Convergent targeting of a common host protein-network by pathogen effectors from three kingdoms of life, Cell Host Microbe 16 (2014) 364–375, https://doi.org/10.1016/j.chom.2014.08.004.
[16] Q. Shen, Y. Liu, N.I. Naqvi, Fungal effectors at the crossroads of phytohormone signaling, Curr. Opin. Microbiol. 46 (2018) 1–6, https://doi.org/10.1016/j.mib.2018.01.006.
[17] A. König, R. Müller, S. Mogavero, B. Hube, Fungal factors involved in host immune evasion, modulation and exploitation during infection, Cell Microbiol. 23 (2021) e13272, https://doi.org/10.1111/cmi.13272.
[18] N.A. Abdul Malik, I.S. Kumar, K. Nadarajah, Elicitor and receptor molecules: orchestrators of plant defense and immunity, Int. J. Mol. Sci. 21 (2020), https://doi.org/10.3390/ijms21030963.
[19] S. Bourras, K.E. McNally, R. Ben-David, F. Parlange, S. Roffler, C.R. Praz, S. Oberhaensli, F. Menardo, D. Stirnweis, Z. Frenkel, L.K. Schaefer, S. Flückiger, G. Treier, G. Herren, A.B. Korol, T. Wicker, B. Keller, Multiple avirulence loci and allele-specific effector recognition control the Pm3 race-specific resistance of wheat to powdery mildew, Plant Cell 27 (2015) 2991–3012, https://doi.org/10.1105/tpc.15.00171.
[20] P.M. Houterman, B.J.C. Cornelissen, M. Rep, Suppression of plant resistance gene-based immunity by a fungal effector, PLoS Pathog. 4 (2008) e1000061, https://doi.org/10.1371/journal.ppat.1000061.
[21] B.J. Condon, Y. Leng, D. Wu, K.E. Bushley, R.A. Ohm, R. Otillar, J. Martin, W. Schackwitz, J. Grimwood, N. MohdZainudin, C. Xue, R. Wang, V.A. Manning, B. Dhillon, Z.J. Tu, B.J. Steffenson, A. Salamov, H. Sun, S. Lowry, K. LaButti, J. Han, A. Copeland, E. Lindquist, K. Barry, J. Schmutz, S.E. Baker, L.M. Ciuffetti, I. V Grigoriev, S. Zhong, B.G. Turgeon, Comparative genome structure, secondary metabolite, and effector coding capacity across Cochliobolus pathogens, PLoS Genet. 9 (2013) e1003233, https://doi.org/10.1371/journal.pgen.1003233.
[22] G.M. Pathak, G.S. Gurjar, N.Y. Kadoo, Insights of *Bipolaris sorokiniana* secretome - an in silico approach, Biologia 75 (2020) 2367–2381, https://doi.org/10.2478/s11756-020-00537-4.
[23] S. Navathe, P.S. Yadav, R. Chand, V.K. Mishra, N.K. Vasistha, P.K. Meher, A. K. Joshi, P.K. Gupta, ToxA-Tsn1 interaction for spot blotch susceptibility in Indian wheat: an example of inverse gene-for-gene relationship, Plant Dis. 104 (2020) 71–81, https://doi.org/10.1094/PDIS-05-19-1066-RE.
[24] W. Zhang, H. Li, L. Wang, S. Xie, Y. Zhang, R. Kang, M. Zhang, P. Zhang, Y. Li, Y. Hu, M. Wang, L. Chen, H. Yuan, S. Ding, H. Li, A novel effector, CsSp1, from *Bipolaris sorokiniana,* is essential for colonization in wheat and is also involved in triggering host immunity, Mol. Plant Pathol. 23 (2022) 218–236, https://doi.org/10.1111/mpp.13155.
[25] M.C. McDonald, D. Ahren, S. Simpfendorfer, A. Milgate, P.S. Solomon, The discovery of the virulence gene ToxA in the wheat and barley pathogen *Bipolaris sorokiniana*, Mol. Plant Pathol. 19 (2018) 432–439, https://doi.org/10.1111/mpp.12535.
[26] B. Mansoori, S. Rajaei, Reactions of some wheat advanced lines and commercial cultivars to common fungal diseases in fars province, Seed Plant J 22 (2006) 455–472, https://doi.org/10.22092/spij.2017.110698.
[27] J.D. Bendtsen, H. Nielsen, G. von Heijne, S. Brunak, Improved prediction of signal peptides: SignalP 3.0, J. Mol. Biol. 340 (2004) 783–795, https://doi.org/10.1016/j.jmb.2004.05.028.
[28] B.-J. Yoon, Hidden Markov models and their applications in biological sequence analysis, Curr. Genom. 10 (2009) 402–415, https://doi.org/10.2174/138920209789177575.
[29] O. Emanuelsson, H. Nielsen, S. Brunak, G. von Heijne, Predicting subcellular localization of proteins based on their N-terminal amino acid sequence, J. Mol. Biol. 300 (2000) 1005–1016, https://doi.org/10.1006/jmbi.2000.3903.

[30] A. Krogh, B. Larsson, G. von Heijne, E.L. Sonnhammer, Predicting transmembrane protein topology with a hidden Markov model: application to complete genomes, J. Mol. Biol. 305 (2001) 567–580, https://doi.org/10.1006/jmbi.2000.4315.
[31] A. Pierleoni, P.L. Martelli, R. Casadio, PredGPI: a GPI-anchor predictor, BMC Bioinf. 9 (2008) 392, https://doi.org/10.1186/1471-2105-9-392.
[32] J. Mistry, S. Chuguransky, L. Williams, M. Qureshi, G.A. Salazar, E.L. L. Sonnhammer, S.C.E. Tosatto, L. Paladin, S. Raj, L.J. Richardson, R.D. Finn, A. Bateman, Pfam: the protein families database in 2021, Nucleic Acids Res. 49 (2021) D412–D419, https://doi.org/10.1093/nar/gkaa913.
[33] S. Hunter, R. Apweiler, T.K. Attwood, A. Bairoch, A. Bateman, D. Binns, P. Bork, U. Das, L. Daugherty, L. Duquenne, R.D. Finn, J. Gough, D. Haft, N. Hulo, D. Kahn, E. Kelly, A. Laugraud, I. Letunic, D. Lonsdale, R. Lopez, M. Madera, J. Maslen, C. McAnulla, J. McDowall, J. Mistry, A. Mitchell, N. Mulder, D. Natale, C. Orengo, A.F. Quinn, J.D. Selengut, C.J.A. Sigrist, M. Thimma, P.D. Thomas, F. Valentin, D. Wilson, C.H. Wu, C. Yeats, InterPro: the integrative protein signature database, Nucleic Acids Res. 37 (2009) D211–D215, https://doi.org/10.1093/nar/gkn785.
[34] J. Sperschneider, P.N. Dodds, D.M. Gardiner, K.B. Singh, J.M. Taylor, Improved prediction of fungal effector proteins from secretomes with EffectorP 2.0, Mol. Plant Pathol. 19 (2018) 2094–2110, https://doi.org/10.1111/mpp.12682.
[35] J. Sperschneider, A.-M. Catanzariti, K. DeBoer, B. Petre, D.M. Gardiner, K.B. Singh, P.N. Dodds, J.M. Taylor, LOCALIZER: subcellular localization prediction of both plant and effector proteins in the plant cell, Sci. Rep. 7 (2017) 44598, https://doi.org/10.1038/srep44598.
[36] R. Kang, Y. Hu, L. Wang, S. Xie, Y. Li, H. Yuan, M. Wang, L. Chen, S. Ding, H. Li, Pathogenicity variation and DNA polymorphism of *Bipolaris sorokiniana* infecting winter wheat in the Huanghuai floodplain of China, Plant Pathol. 70 (2021) 87–99, https://doi.org/10.1111/ppa.13256.
[37] V. Jalili, E. Afgan, Q. Gu, D. Clements, D. Blankenberg, J. Goecks, J. Taylor, A. Nekrutenko, The Galaxy platform for accessible, reproducible and collaborative biomedical analyses: 2020 update, Nucleic Acids Res. 48 (2020) W395–W402, https://doi.org/10.1093/nar/gkaa434.
[38] A.M. Bolger, M. Lohse, B. Usadel, Trimmomatic: a flexible trimmer for Illumina sequence data, Bioinformatics 30 (2014) 2114–2120, https://doi.org/10.1093/bioinformatics/btu170.
[39] A. Dobin, C.A. Davis, F. Schlesinger, J. Drenkow, C. Zaleski, S. Jha, P. Batut, M. Chaisson, T.R. Gingeras, STAR: ultrafast universal RNA-seq aligner, Bioinformatics 29 (2013) 15–21, https://doi.org/10.1093/bioinformatics/bts635.
[40] M. Pertea, G.M. Pertea, C.M. Antonescu, T.-C. Chang, J.T. Mendell, S.L. Salzberg, StringTie enables improved reconstruction of a transcriptome from RNA-seq reads, Nat. Biotechnol. 33 (2015) 290–295, https://doi.org/10.1038/nbt.3122.
[41] V. Jiménez-Jacinto, A. Sanchez-Flores, L. Vega-Alvarado, Integrative differential expression analysis for multiple EXperiments (IDEAMEX): a web server tool for integrated RNA-seq data analysis, Front. Genet. 10 (2019) 279, https://doi.org/10.3389/fgene.2019.00279.
[42] M.I. Love, W. Huber, S. Anders, Moderated estimation of fold change and dispersion for RNA-seq data with DESeq2, Genome Biol. 15 (2014) 550, https://doi.org/10.1186/s13059-014-0550-8.
[43] L. Wang, J.P. Stegemann, Extraction of high quality RNA from polysaccharide matrices using cetyltrimethylammonium bromide, Biomaterials 31 (2010) 1612–1618, https://doi.org/10.1016/j.biomaterials.2009.11.024.
[44] X. Rao, X. Huang, Z. Zhou, X. Lin, An improvement of the 2ˆ(-delta delta CT) method for quantitative real-time polymerase chain reaction data analysis, Biostat. Bioinforma. Biomath. 3 (2013) 71–85.
[45] K.J. Livak, T.D. Schmittgen, Analysis of relative gene expression data using real-time quantitative PCR and the 2-ΔΔCT method, Methods 25 (2001) 402–408, https://doi.org/10.1006/meth.2001.1262.
[46] L. Holm, Using Dali for protein structure comparison, Methods Mol. Biol. 2112 (2020) 29–42, https://doi.org/10.1007/978-1-0716-0270-6_3.
[47] I.N. Shindyalov, P.E. Bourne, Protein structure alignment by incremental combinatorial extension (CE) of the optimal path, Protein Eng. 11 (1998) 739–747, https://doi.org/10.1093/protein/11.9.739.
[48] Y. Zhang, J. Skolnick, TM-align: a protein structure alignment algorithm based on the TM-score, Nucleic Acids Res. 33 (2005) 2302–2309, https://doi.org/10.1093/nar/gki524.
[49] R. Ayoub, Y. Lee, RUPEE: a fast and accurate purely geometric protein structure search, PLoS One 14 (2019) e0213712, https://doi.org/10.1371/journal.pone.0213712.
[50] R. Ayoub, Y. Lee, Protein structure search to support the development of protein structure prediction methods, Proteins 89 (2021) 648–658, https://doi.org/10.1002/prot.26048.
[51] J.-M. Chandonia, N.K. Fox, S.E. Brenner, SCOPe: classification of large macromolecular structures in the structural classification of proteins-extended database, Nucleic Acids Res. 47 (2019) D475–D481, https://doi.org/10.1093/nar/gky1134.
[52] M. Alkan, H. Bayraktar, M. İmren, F. Özdemir, R. Lahlali, F. Mokrini, T. Paulitz, A. A. Dababat, G. Özer, Monitoring of host suitability and defense-related genes in wheat to *Bipolaris sorokiniana*, J. Fungi (Basel, Switzerland) 8 (2022), https://doi.org/10.3390/jof8020149.
[53] S. Aditya, R. Aggarwal, B.M. Bashyal, M.S. Gurjar, M.S. Saharan, S. Aggarwal, Unraveling the dynamics of wheat leaf blight complex: isolation, characterization, and insights into pathogen population under Indian conditions, Front. Microbiol. 15 (2024) 1287721, https://doi.org/10.3389/fmicb.2024.1287721.
[54] A.R. Cortázar, A.M. Aransay, M. Alfaro, J.A. Oguiza, J.L. Lavín, SECRETOOL: integrated secretome analysis tool for fungi, Amino Acids 46 (2014) 471–473, https://doi.org/10.1007/s00726-013-1649-z.
[55] J. Choi, J. Park, D. Kim, K. Jung, S. Kang, Y.-H. Lee, Fungal Secretome Database: integrated platform for annotation of fungal secretomes, BMC Genom. 11 (2010) 105, https://doi.org/10.1186/1471-2164-11-105.
[56] G. Lum, X.J. Min, FunSecKB: the fungal secretome KnowledgeBase, Database 2011 (2011) bar001, https://doi.org/10.1093/database/bar001.
[57] J. Meinken, D.K. Asch, K.A. Neizer-Ashun, G.-H. Chang, C.R. Cooper JR., X.J. Min, FunSecKB2: a fungal protein subcellular location knowledgebase, Comput. Mol. Biol. 4 (2014).
[58] R.P. Vivek-Ananth, K. Mohanraj, M. Vandanashree, A. Jhingran, J.P. Craig, A. Samal, Comparative systems analysis of the secretome of the opportunistic pathogen *Aspergillus fumigatus* and other Aspergillus species, Sci. Rep. 8 (2018) 6617, https://doi.org/10.1038/s41598-018-25016-4.
[59] O. Mueller, R. Kahmann, G. Aguilar, B. Trejo-Aguilar, A. Wu, R.P. de Vries, The secretome of the maize pathogen *Ustilago maydis*, Fungal Genet. Biol. 45 (Suppl 1) (2008) S63–S70, https://doi.org/10.1016/j.fgb.2008.03.012.
[60] A. Morais do Amaral, J. Antoniw, J.J. Rudd, K.E. Hammond-Kosack, Defining the predicted protein secretome of the fungal wheat leaf pathogen *Mycosphaerella graminicola*, PLoS One 7 (2012) e49904, https://doi.org/10.1371/journal.pone.0049904.
[61] S.F. Altschul, T.L. Madden, A.A. Schäffer, J. Zhang, Z. Zhang, W. Miller, D. J. Lipman, Gapped BLAST and PSI-BLAST: a new generation of protein database search programs, Nucleic Acids Res. 25 (1997) 3389–3402, https://doi.org/10.1093/nar/25.17.3389.
[62] C.J. Ridout, P. Skamnioti, O. Porritt, S. Sacristan, J.D.G. Jones, J.K.M. Brown, Multiple avirulence paralogues in cereal powdery mildew fungi may contribute to parasite fitness and defeat of plant resistance, Plant Cell 18 (2006) 2402–2414, https://doi.org/10.1105/tpc.106.043307.
[63] Y. Cao, F. Kümmel, E. Logemann, J.M. Gebauer, A.W. Lawson, D. Yu, M. Uthoff, B. Keller, J. Jirschitzka, U. Baumann, K. Tsuda, J. Chai, P. Schulze-Lefert, Structural polymorphisms within a common powdery mildew effector scaffold as a driver of coevolution with cereal immune receptors, Proc. Natl. Acad. Sci. U.S.A. 120 (2023) e2307604120, https://doi.org/10.1073/pnas.2307604120.
[64] C. Pedersen, E. Ver Loren van Themaat, L.J. McGuffin, J.C. Abbott, T.A. Burgis, G. Barton, L. V Bindschedler, X. Lu, T. Maekawa, R. Wessling, R. Cramer, H. Thordal-Christensen, R. Panstruga, P.D. Spanu, Structure and evolution of barley powdery mildew effector candidates, BMC Genom. 13 (2012) 694, https://doi.org/10.1186/1471-2164-13-694.
[65] M.D. Bolton, H.P. van Esse, J.H. Vossen, R. de Jonge, I. Stergiopoulos, I.J. E. Stulemeijer, G.C.M. van den Berg, O. Borrás-Hidalgo, H.L. Dekker, C.G. de Koster, P.J.G.M. de Wit, M.H.A.J. Joosten, B.P.H.J. Thomma, The novel Cladosporium fulvum lysin motif effector Ecp6 is a virulence factor with orthologues in other fungal species, Mol. Microbiol. 69 (2008) 119–136, https://doi.org/10.1111/j.1365-2958.2008.06270.x.
[66] R. de Jonge, H.P. van Esse, A. Kombrink, T. Shinya, Y. Desaki, R. Bours, S. van der Krol, N. Shibuya, M.H.A.J. Joosten, B.P.H.J. Thomma, Conserved fungal LysM effector Ecp6 prevents chitin-triggered immunity in plants, Science 329 (2010) 953–955, https://doi.org/10.1126/science.1190859.
[67] A. Sánchez-Vallet, R. Saleem-Batcha, A. Kombrink, G. Hansen, D.-J. Valkenburg, B. P.H.J. Thomma, J.R. Mesters, Fungal effector Ecp6 outcompetes host immune receptor for chitin binding through intrachain LysM dimerization, Elife 2 (2013) e00790, https://doi.org/10.7554/eLife.00790.
[68] C.H. Mesarich, I. Barnes, E.L. Bradley, S. de la Rosa, P.J.G.M. de Wit, Y. Guo, S. A. Griffiths, R.C. Hamelin, M.H.A.J. Joosten, M. Lu, H.M. McCarthy, C.R. Schol, I. Stergiopoulos, M. Tarallo, A.Z. Zaccaron, R.E. Bradshaw, Beyond the genomes of *Fulvia fulva* (syn. *Cladosporium fulvum*) and *Dothistroma septosporum*: new insights into how these fungal pathogens interact with their host plants, Mol. Plant Pathol. 24 (2023) 474–494, https://doi.org/10.1111/mpp.13309.
[69] H.P. van Esse, M.D. Bolton, I. Stergiopoulos, P.J.G.M. de Wit, B.P.H.J. Thomma, The chitin-binding *Cladosporium fulvum* effector protein Avr4 is a virulence factor, Mol. Plant Microbe Interact. 20 (2007) 1092–1101, https://doi.org/10.1094/MPMI-20-9-1092.
[70] R. de Jonge, B.P.H.J. Thomma, Fungal LysM effectors: extinguishers of host immunity? Trends Microbiol. 17 (2009) 151–157, https://doi.org/10.1016/j.tim.2009.01.002.
[71] H.A. van den Burg, S.J. Harrison, M.H.A.J. Joosten, J. Vervoort, P.J.G.M. de Wit, *Cladosporium fulvum* Avr4 protects fungal cell walls against hydrolysis by plant chitinases accumulating during infection, Mol. Plant Microbe Interact. 19 (2006) 1420–1430, https://doi.org/10.1094/MPMI-19-1420.
[72] M. Rep, M. Meijer, P.M. Houterman, H.C. van der Does, B.J.C. Cornelissen, *Fusarium oxysporum* evades I-3-mediated resistance without altering the matching avirulence gene, Mol. Plant Microbe Interact. 18 (2005) 15–23, https://doi.org/10.1094/MPMI-18-0015.
[73] H.C. van der Does, R.G.E. Duyvesteijn, P.M. Goltstein, C.C.N. van Schie, E.M. M. Manders, B.J.C. Cornelissen, M. Rep, Expression of effector gene SIX1 of *Fusarium oxysporum* requires living plant cells, Fungal Genet. Biol. 45 (2008) 1257–1264, https://doi.org/10.1016/j.fgb.2008.06.002.
[74] K. Seong, K. V Krasileva, Prediction of effector protein structures from fungal phytopathogens enables evolutionary analyses, Nat. Microbiol. 8 (2023) 174–187, https://doi.org/10.1038/s41564-022-01287-6.
[75] D.S. Yu, M.A. Outram, A. Smith, C.L. McCombe, P.B. Khambalkar, S.A. Rima, X. Sun, L. Ma, D.J. Ericsson, D.A. Jones, S.J. Williams, The structural repertoire of *Fusarium oxysporum* f. sp. lycopersici effectors revealed by experimental and computational studies, Elife 12 (2024), https://doi.org/10.7554/eLife.89280.